CSIRO Publishing
www.publish.csiro.au/journals/rs

The Royal Society of Victoria, 132, 49–64, 2020
10.1071/RS20004

REVISITING THE 1888 CENTENNIAL DROUGHT

Mathilde E.H. Ritman[1,2], Linden C. Ashcroft[1,2]

[1]School of Earth Sciences, University of Melbourne, Victoria 3010, Australia
[2]Australian Centre of Excellence for Climate Extremes, University of Melbourne, Victoria 3010, Australia

Correspondence: Mathilde Ritman, mritman@student.unimelb.edu.au

ABSTRACT: Droughts are a key feature of Australia's climate and can lead to water shortages, crop failure and economic instability. Historical droughts are an important source of information to better understand recent droughts and how they might be managed. However, the majority of studies into Australian drought only consider dry periods in the 20th and 21st centuries. Here, a newly developed gridded rainfall dataset from the Bureau of Meteorology and a network of historical rainfall stations are used to re-examine the short but sharp Centennial Drought of 1888. The Centennial Drought is explored on a monthly scale, highlighting key periods of rainfall deficiency, and identifying the impacts of relevant atmospheric circulation patterns. The most significant rainfall declines occur in autumn and spring and are likely to be the result of an El Niño event, a positive Sub-Tropical Ridge intensity anomaly, and seasonal fluctuations of the Southern Annular Mode. Comparing the Centennial Drought to other short droughts of 1914–15, 1982–83 and 2017~ indicates that the magnitude of the rainfall deficiencies and widespread spatial extent are comparable, placing the Centennial Drought alongside some of the most severe short droughts in Australia's colonial climate history.

Keywords: drought, climate, gridded climate data, historic climatology, southeastern Australia, Centennial Drought 1888

DROUGHT IN SOUTHEASTERN AUSTRALIA

Recently, large regions of southeastern Australia (SEA) have experienced very much below-average, long-term rainfall declines and severely limited water resources. The year 2019 was the driest on record for Australia, and the 34-month period from January 2017 to October 2019 was the driest on record for New South Wales and the Murray–Darling Basin (records beginning in 1900; Bureau of Meteorology 2019). While good rainfall in 2020 has provided relief to many drought-affected regions of SEA, water storages of the Northern Basin remain low, and, at the time of writing, long-term rainfall deficiencies persist in northern New South Wales and southern Queensland (Bureau of Meteorology 2020a). The evolution and severity of drought in SEA is influenced by a range of meteorological and climatological factors, including the El Niño – Southern Oscillation (ENSO), the Indian Ocean Dipole (IOD), the Southern Annular Mode (SAM) and the Sub-Tropical Ridge (STR) (Murphy & Timbal 2008).

ENSO is a primary driver of interannual rainfall variability in SEA (Dey et al. 2019; Nicholls 1987, 1989), modulating precipitation most significantly in winter and spring (McBride & Nicholls 1983; Risbey et al. 2009; Verdon-Kidd & Kiem 2009). An El Niño event corresponds to negative sea surface temperature (SST) anomalies in the west Pacific Ocean and generally results in reduced rainfall and drought conditions across eastern Australia (Power et al. 1998).

The IOD describes SST anomalies in the Indian Ocean and influences rainfall patterns in southern Australia between June and October (Ashok et al. 2003; Saji et al. 1999). A negative IOD phase describes warm SST anomalies to the northwest of Australia, typically increasing the progression of tropical moisture and rainfall into SEA. However, the effects of the IOD and ENSO are not entirely independent (Li et al. 2016; Meyers et al. 2007; Nicholls 1989, 2010; Risbey et al. 2009; Verdon-Kidd & Franks 2005).

The SAM is a dominant driver of extratropical rainfall variability in the southern hemisphere and describes the north–south latitudinal progression of zonal wind anomalies between approximately 30° and 60° south (Hendon et al. 2007; Thompson & Solomon 2002). SAM phases oscillate on time scales of weeks to months and their impacts on rainfall vary seasonally. In SEA, a negative phase SAM in winter and spring indicates the northward progression of the westerly wind belt and is attributed to reduced rainfall across coastal New South Wales and increased rainfall in southern Victoria and Tasmania (Hendon et al. 2007; Kiem & Verdon-Kidd 2010).

The intensity and latitude of the STR, a quasi-stationary belt of mid-latitude anticyclones, is also known to modulate precipitation in SEA (Drosdowsky 2005; Timbal & Drosdowsky 2013). The 'belt' corresponds to the descending branch of the Hadley Circulation Cell and manifests a global band of increased surface pressure that oscillates north–south seasonally at around 30° south

(Allan & Haylock 1993; Larsen & Nicholls 2009). Positive STR intensity (STR-I) anomalies can suppress the intrusion of frontal systems in SEA and are associated with reduced precipitation in the region from autumn to spring (Timbal & Drosdowsky 2013).

The complex influences of these large-scale drivers, along with other meteorological and geographical factors (e.g. Holgate et al. 2020), means that every drought experienced in Australia is unique. The majority of studies focus on multi-year drought events, such as the Federation (1895–1903), World War II (1939–1945) and Millennium droughts (1997–2009) (Murphy & Timbal 2008; Ummenhofer et al. 2009; Verdon-Kidd & Kiem 2009). However, short droughts can also have devastating impacts on farming, ecosystems and the economy.

The 1982–83 drought event, for example, saw national wheat production fall to 63% of the previous five-year average, and the net value of rural production was estimated to be 56% of that seen in the previous four years. Similarly, in 1914, during the 1914–15 drought, Western Australia recorded its lowest wheat yield of the century thus far (Gibbs 1984; Bureau of Meteorology 2020b).

Most studies exploring historical droughts in Australia are limited to the 20th and 21st centuries, as this is the period when national datasets are available for analysis. While there are some studies examining 19th century rainfall variability (e.g. Gergis & Ashcroft 2013; Timbal & Fawcett 2013; Verdon-Kidd & Kiem 2009), they are often based only on weather station observations rather than a temporally consistent, gridded product for the pre-1900 period. This means that 19th century droughts in documentary records (e.g. Fenby & Gergis 2013; Helman 2009) are not included in quantitative studies that aim to improve understanding and predictability of drought onset and severity.

This study aims to address the lack of modern analysis of historical droughts by re-examining the seasonality, spatial footprint and possible causes of the short but sharp 1888 Centennial Drought in SEA. We make use of a newly developed, gridded product from the Bureau of Meteorology (Evans et al. 2020) that extends back to 1880, as well as historic station-based observations (Gergis & Ashcroft 2013). Together, these datasets are used to detail the evolution of the Centennial Drought on the monthly scale, as well as to provide a description of the drought's regional signature on this timescale throughout SEA. In addition to historic rainfall data, climate indices data on the monthly and quarterly scales are also used. By considering the oscillations of these climate indices and the circulation features they represent, the climatic features and possible causes of the Centennial Drought in 1888 are explored.

Following the quantitative analysis of the Centennial Drought, three other significant short droughts of Australia's climate history are introduced — the 1914–15 and 1982–83 droughts and the most recent drought, from 2017 and ongoing (at the time of publication). The monthly evolution, severity, and circulation feature variability of these droughts are contrasted with the conditions of 1888, providing context for the magnitude of the recorded rainfall declines and the resulting impacts on the Australian communities. We decided to use both datasets for the historic analysis in order to provide additional discussion on the agreement between the two on the monthly scale, highlighting the ability, and limitations, of each in conducting historical climate analyses.

THE CENTENNIAL DROUGHT

The Centennial Drought was reported in historical records as a short, severe drought that affected large regions of SEA throughout 1888. Indeed, previous discussion of the drought suggests it may have been the worst endured by the Australian communities at the time and its impacts unrivalled (Figure 1; Gibbs & Maher 1967; Nicholls 1997). However, the detailed nature of the drought and how it compares with other short events have not been explored using modern datasets. Recently recovered daily precipitation observations from Eversleigh in the New England region of New South Wales (NSW), show that 1888 was the driest year of the 46 recorded between 1877 and 1922 (Bridgman et al. 2019), with annual totals at less than 40% of the recorded long-term average.

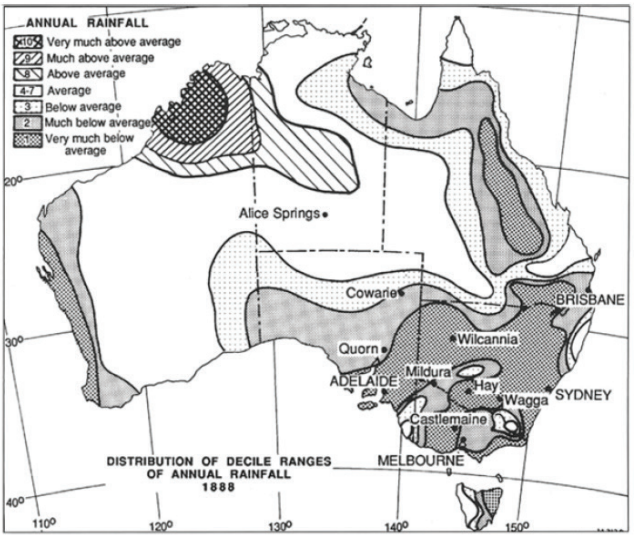

Figure 1: Interpolated distribution of annual Australian rainfall anomalies for 1888, as adapted from Gibbs and Maher (1967) by Nicholls (1997).

As explained by Nicholls (1997), the impacts of the sudden and extreme drying on the colonies were compounded by the strong dependence on agriculture and the devastating lack of relief strategies at the time. Crops failed in massive proportions and the NSW wheat yield for

1888 was less than a third of the annual average for the decade. Livestock in the order of millions were starved, with the owner of one station reported to have cut the throats of 25,000 sheep in an attempt to preserve feed. Native fauna disappeared from regions where they were previously common, locust swarms added to the desolation, and a large class of dispossessed farmers appeared, having been forced to abandon their properties.

One poem published in the *Gippsland Farmers' Journal* during the drought further highlights the extreme impact the drought had on the communities at the time: 'The earth was brown, the sky was blue, No moisture fell, no drop of dew. … There a grey toad all parched and dead, Stuck in a crack with blistered head' (Glenmaggie 1888).

DATA AND METHODS

Precipitation data

Monthly precipitation data are sourced from two datasets: a 42-station network of historical instrumental precipitation records from across SEA (Gergis & Ashcroft 2013), and the Bureau of Meteorology's interpolated monthly precipitation dataset, using a subset extracted across SEA for the period since 1880 (Evans et al. 2020), henceforth referred to as the Australian Gridded Climate Data (AGCD).

The AGCD analysis extends the historic reach of high-resolution gridded climate data by 20 years, with monthly interpolated data beginning in 1880 compared with 1900 for the currently operational gridded dataset, the Australian Water Availability Project (AWAP) (Jones et al. 2009). The AGCD dataset is also resolved to the higher 0.01° by 0.01° grids, where AWAP is resolved to 0.05° by 0.05° grids, and achieves a significant reduction in interpolation errors and biases for the period 1900 to 2018 (Evans et al. 2020).

For this study, SEA is defined as the land between 44.5–27° south and 135–156.25° east. This area was selected as it is well covered by monthly data in the late 19th century (Evans et al. 2020, figure 4). AGCD uses monthly data taken from the Bureau of Meteorology's Australian Data Archive for Meteorology database (ADAM, http://www.bom.gov.au/climate/cdo/images/about/ADAM.pdf). The number of stations used nationally ranges from around 500 in 1880 to more than 7000 in the 1960s and 1970s. Data from around 1500 stations are used in the 1888 grids, with the majority of these located in SEA.

The station network from Gergis and Ashcroft (2013) comprises long-term monthly precipitation from ADAM. Combined, the stations span the years 1850–2009; however, not all stations have temporally consistent data for this period. Figure 2 shows the locations of the 42 long-term rainfall stations from the station network used in this research.

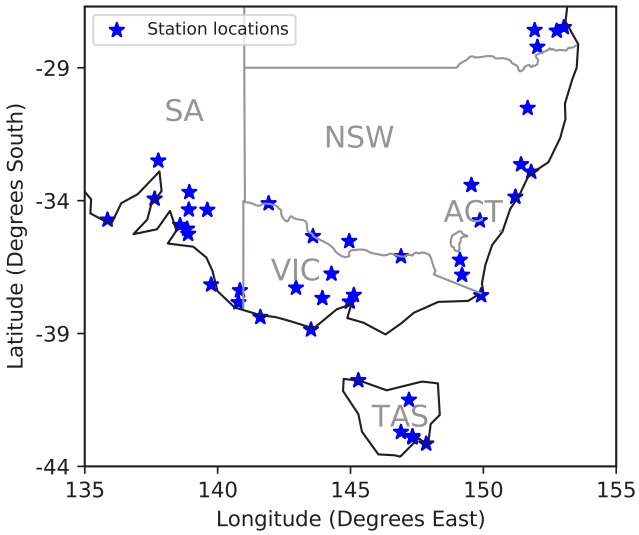

Figure 2: Geographic locations of the 42-historic stations used in this research.

It is important to note that the gridded and station-based datasets are not completely independent. Monthly precipitation data from the AGCD product are based on all available monthly station data, including — but not limited to — those which also exist in the historical station network of Gergis and Ashcroft (2013). Despite this, numerous factors distinguish the two datasets, resulting in the potential for a greater range of disagreement between the two than might otherwise be anticipated. The AGCD employs automated quality control of the monthly data based on the statistical interpolation analysis procedure, which involves identification, cross-validation and removal of probabilistic data errors. On the other hand, the station network from Gergis and Ashcroft (2013) was subject to extensive manual quality control, using archived station history information from the Bureau of Meteorology.

Precipitation anomalies for both datasets were calculated with respect to the 78-year period 1888–1965, as this was the longest period for which the 42 stations in the network had largely consistent monthly data. Only two stations do not have complete data for this period: Strathalbyn in South Australia (Bureau of Meteorology station number 023747) is missing 26 years of data between 1901 and 1927, and Mount Nelson in Tasmania (Bureau of Meteorology station number 094045) is missing four years between 1905 and 1909.

For the AGCD, many more stations are included over the full period used for the 78-year climatology, including stations with a relatively short record, or a record that continues beyond 1965. As a result, while there may be

small differences in the rainfall totals for just 1888, the anomalies with reference to the 78-year period can exhibit larger differences. The calculation of two different long-term climatologies provides an additional difference between the two datasets.

Monthly precipitation anomalies were calculated for a given station (for the 42-station network) or grid point (for AGCD) relative to the climatology period 1888–1965. Area-averages for SEA were calculated by taking the arithmetic mean of these anomalies across each grid point or station value.

Table 1: Climate indices data details. The Southern Oscillation Index (SOI) and Niño 3.4 indices indicate the development of an El Niño event. The Dipole Mode Index (DMI) and South Eastern Indian Ocean (SEOI) indicate the phase of the Indian Ocean Dipole. The Southern Annular Mode (SAM) indicates the meridional progression of the westerly wind belt in the Southern Ocean. The Sub-Tropical Ridge intensity (STR-I) indicates the magnitude of the quasi-stationary high pressure belt in the subtropics.

Data	Frequency	Climatology	Source; methods
SOI	Monthly	1933-1992	Bureau of Meteorology 2019c
Niño 3.4	Monthly	1961-1990	HadISST; Rayner et al. 2003
DMI	Monthly	NA	HadISST; Rayner et al. 2003
SEIO	Monthly	1971-2000	ERSST; climexp.knmi.nl
SAM	Quarterly	NA	Visbeck 2009
SAM	Monthly	1981-2010	20CRV2c; Gong & Wang 1999
STRI	Monthly	NA	Pepler, Ashcroft & Trewin 2018

Climate indices data

Monthly Southern Oscillation Index (SOI) data were sourced from the Bureau of Meteorology as a representation of atmospheric ENSO variability, where data were calculated relative to the period 1933 to 1992 inclusive. Anomalies in the Niño 3.4 region (-5–5º south, 170–120º west) derived from the Hadley Centre Sea Ice and Sea Surface Temperature dataset (HadISST) were used to capture the equatorial Pacific Ocean temperature variations (Trenberth & National Center for Atmospheric Research Staff 2019).

The Dipole Mode Index (DMI) is a measure of the difference in SST between the western (50–70º east) and eastern (90–110º east) equatorial (10º north – 10º south) Indian Ocean (Saji et al. 1999). Here the DMI is derived from the HadISST dataset using the Royal Netherlands Meteorological Institute Climate Explorer webpage (climexp.knmi.nl). Previous examination of the input data for HadISST showed that coverage is fair from at least 1880 onwards (Rayner et al. 2003). However, the lack of ship-based observations prior to 1958 is argued to significantly reduce the reliability of historic DMI data (Abram et al. 2015; Saji et al. 1999). Another indicator of IOD conditions that is most relevant for Australia is the South Eastern Indian Ocean (SEOI) SST. SEOI data were derived from the NOAA Extended Reconstructed Sea Surface Temperature (ERSST) and were also sourced from climexp.knmi.nl.

Quarterly regional SAM data are from Visbeck (2009) and based on the Global Historical Climatology Network, while monthly SAM data are derived from the 20th century Reanalysis Version 2c (20CRV2c) where they have been calculated according to methods outlined by Gong and Wang (1999). Extended monthly STR intensity (STR-I) data are sourced from Pepler et al. (2018) where it was calculated from the Bureau of Meteorology's mean sea-level pressure (MSLP) station data by the methods outlined by Drosdowsky (2005) and Timbal and Drosdowsky (2013).

Since the climatology periods for the different indices are inconsistent (see Table 1), discussion involving comparison of their absolute values will not be included here. Instead, climate indices data are only contrasted in the relative sense and their individual oscillations considered.

RESULTS

Severity, extent and evolution of the Centennial Drought

The extreme rainfall declines of 1888 place the Centennial Drought as a standout year in SEA's rainfall history (Figure 3). Previous studies by Gibbs and Maher (1967) and Nicholls (1997) depicted the spatial extent of the Centennial Drought, relative to rainfall data available between 1885 and 1965, applied to the whole of Australia (see Figure 1). The historical examination shows the most extreme rainfall deficiencies across SEA, a thin region of inland coastal Queensland and far west Western Australia. Figure 4 depicts a similar result using AGCD (Evans et al. 2020, their figure 19).

Predictably, the best agreement between the historical map and modern analysis occurs where historical stations are most abundant, as the historical map would also have drawn on these observations. The declines observed in eastern Queensland, the west coast of Western Australia and northeast South Australia are also represented by the AGCD, though are less pronounced in severity and spatial extent than the historical interpretation.

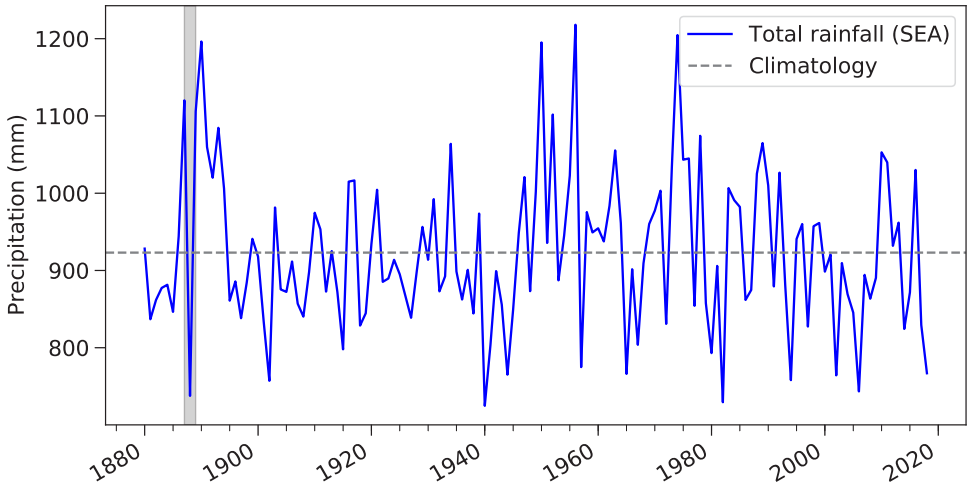

Figure 3: Annual rainfall totals for SEA for the AGCD product (mm). The Centennial Drought 1888 is highlighted in grey, and the 1888–1965 mean is shown by the grey dashed line.

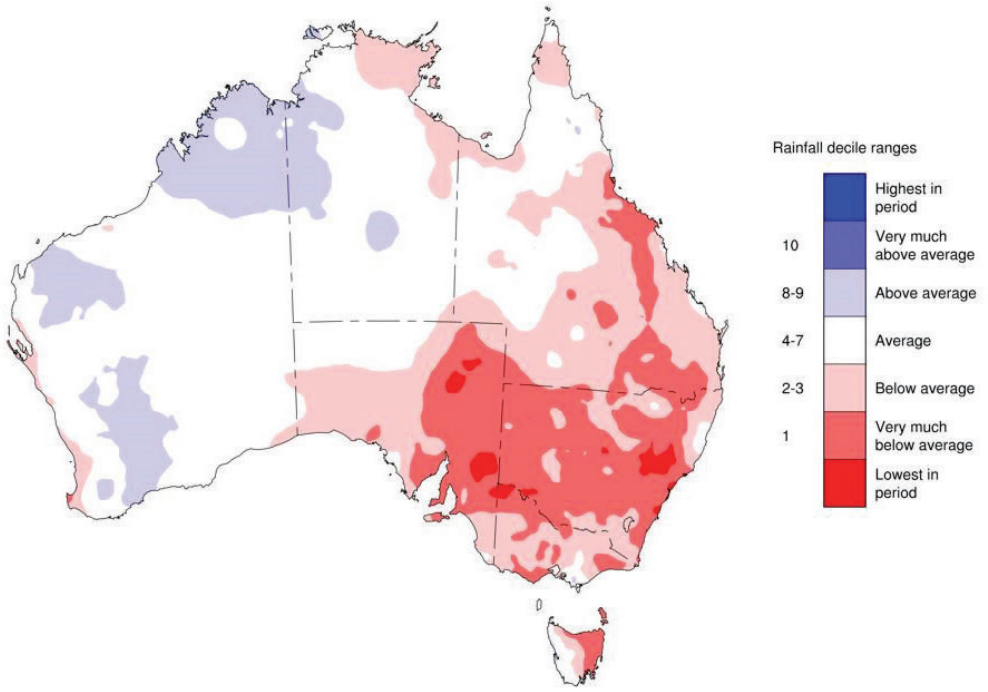

Figure 4: Distribution of annual Australian rainfall deciles for 1888, using the new gridded climate data and relative to the period 1888–1965 (Evans et al. 2020, figure 19).

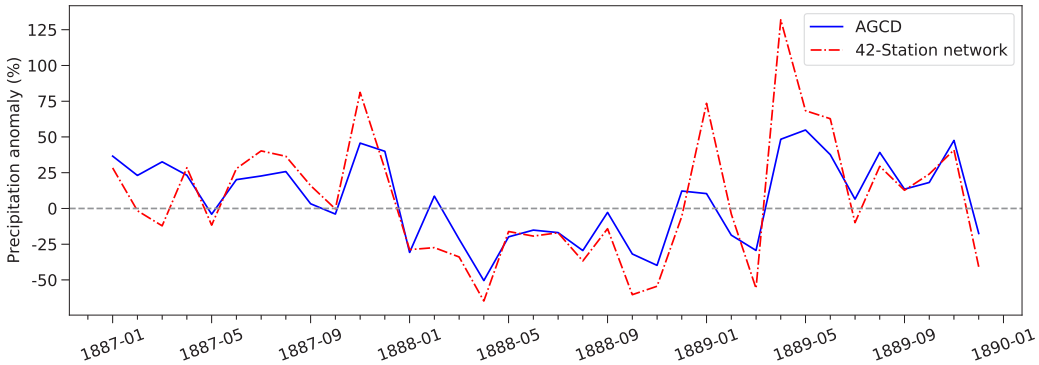

Figure 5: Monthly rainfall anomalies (%) averaged across all locations for the 42-station network (red dashed line) and the gridded climate data (blue solid line) and relative to the period 1888–1965.

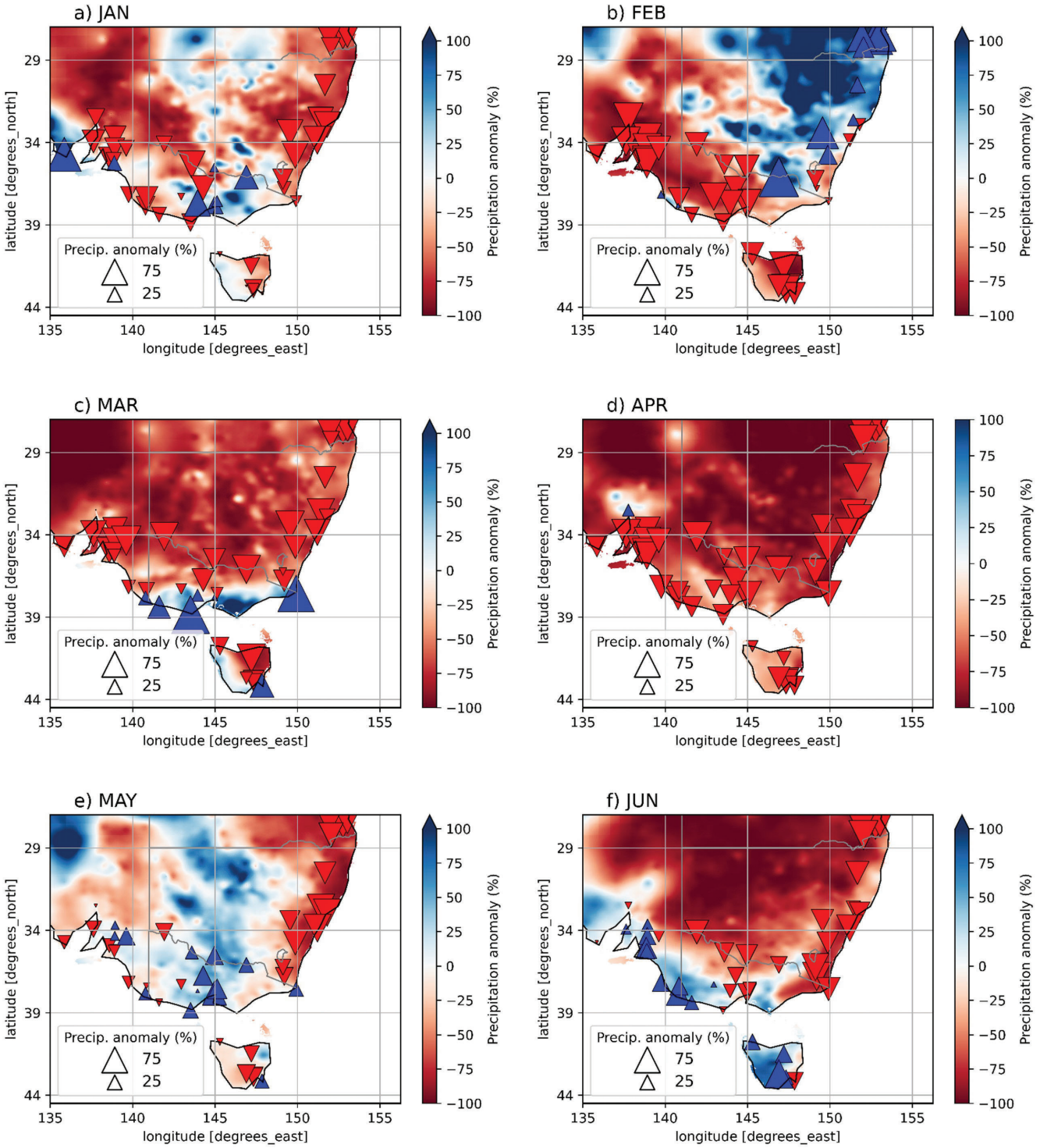

Figures 6a and 6b (opposite page): a) – l) Monthly spatial distribution of rainfall anomalies (%) for January–December 1888 and relative to the period 1888–1965 across southeastern Australia. Triangles represent the 42-station network anomalies, upwards pointing (blue) indicates positive anomalies while downwards pointing (red) represents negative. The relative size of the triangle represents the magnitude of the anomaly. The gridded climate data anomalies are represented in red for below average and blue for above average.

Evolution of the monthly rainfall anomalies (Figure 5) shows that 1887 experienced above average rainfall, particularly later in the year. In November 1887, SEA as a whole received between 45% and 80% more rainfall than the November 1888–1965 average. The descent into drought conditions following the wet warm season was rapid. The station network reports rainfall 30% below average in February 1888, although AGCD reports slightly above average rainfall. Both datasets, however, indicate a sharp decline in rainfall in mid-autumn, with April 1888 being the driest month of the drought for SEA.

Below average rainfall continued throughout winter

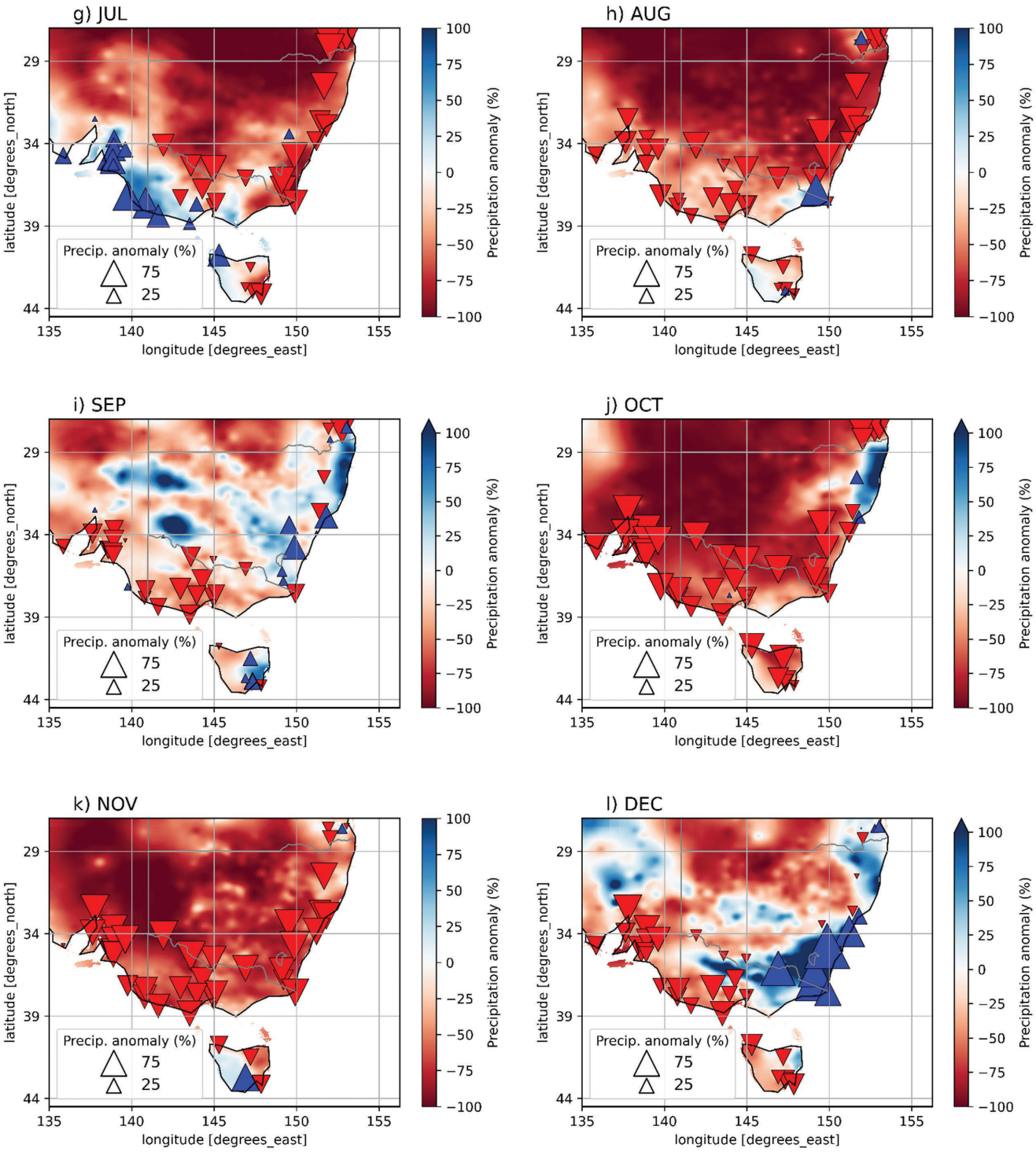

into spring, with both datasets capturing October and November as the next driest months. AGCD indicates rainfall was at least 30% below average at this time, while the 42-station network indicates it was at least 50% below. This discrepancy could result from the coastal bias of the station network, as SEA's coastal regions generally receive greater rainfall totals than those seen inland (Bureau of Meteorology 2020c).

Rainfall began to recover by December 1888, with both datasets reporting SEA precipitation close to average. The year 1889 saw irregular rainfall in the early months, with both January and April being wet, while February and March remained below average. This pattern is particularly distinct in the station network data.

A spatial comparison of the monthly precipitation anomalies observed in the two datasets during the drought year (Figure 6) shows the wide extent of the drought, and indicates that the station network and the AGCD capture similar patterns down to the local level. Four of the twelve months saw large swathes of SEA receiving 25–100% below the 78-year rainfall average, illustrating the severe nature of the drought. Most of the rainfall observed in

February 1888 fell throughout inland NSW and across the northeastern coast, while southwestern Victoria, South Australia and Tasmania experienced significant declines (Figure 6B). According to the AGCD, northeastern inland regions of NSW, west of the Great Dividing Range, saw rainfall between 150% and 300% above average, little of which is captured by the station network due to the historical bias towards coastal observations (Gergis & Ashcroft 2013).

In March (Figure 6C), five southern Victorian stations recorded positive rainfall anomalies, indicating wet conditions across this region, again supported by the AGCD. April was dry across the entire region, while some above average rainfall was received in May in central SEA. Most of SEA was exceptionally dry in June and July (Figures 6F, G) except for a region extending across southeastern South Australia and southwestern Victoria where rainfall was above average. This positive signal is coherent across both datasets, suggesting enhanced westerly winds and associated rain-bearing systems, rather than a data error.

In contrast, August (Figure 6H) experienced widespread rainfall reductions that appear punctuated by positive anomalies in far eastern Victoria and southeastern Queensland. October and November also show widespread rainfall deficits with little spatial variation except for isolated regions where positive rainfall anomalies arise in both datasets. These exceptions to the dominating dry conditions may result from data issues or could indicate localised rainfall events.

Circulation feature variability during the Centennial Drought

Figure 7 depicts the historical climate indices data for the three-year period 1887 to 1889. The data show a significant positive Niño 3.4 anomaly in conjunction with a negative SOI, indicating the development of a short, intense El Niño event from austral winter of 1888 through to autumn 1889.

Both the DMI and the SEOI were close to average throughout 1888. The DMI was largely negative, while the (inverted) SEOI was positive in the first half of 1888 and negative later in the year. The implications of this are conflicting. The DMI indicates the possible development of a negative IOD phase and increased precipitation for SEA, while the SEOI indicates cooler surface waters in the eastern Indian Ocean which would suppress rainfall in SEA. This may result from issues of data quality, outlined previously. Thus, it is possible that the IOD signals at the time of the Centennial Drought are not well represented by these data (Abram et al. 2015; Saji et al. 1999).

On average, the data suggest that 1888 saw a negative SAM phase across the Southern Hemisphere. This is indicated by both the Visbeck and 20CR SAM indices and describes northerly progression of the westerly wind belt that encircles Antarctica. The impacts of this phase on SEA rainfall vary both seasonally and spatially. In the cooler months, the negative SAM is expected to have increased precipitation in southern Victoria and Tasmania and decreased precipitation in coastal New South Wales and southern Queensland (Hendon et al. 2007).

The STR was predominantly above average in intensity throughout 1888, despite relatively large monthly variability with an annual mean anomaly of +1 hPa. In particular, the data show increases in MSLP during April of between 3 and 6 hPa. The positive pressure anomalies suppress rainfall throughout SEA by blocking frontal systems and their associated rain from reaching large regions of southern Australia (Timbal & Drosdowsky 2013).

DISCUSSION

Atmospheric drivers of the Centennial Drought

Table 2: Correlations between precipitation and the relevant climate indices (for details on climate indices, see Table 1).

Data	**Period**	
	IPO positive phase (1880-1888)	Climatology period (1888-1965)
SOI	-0.30	-0.20
Niño 3.4	-0.31	-0.18
DMI	0.32	-0.07
SEIO	-0.36	-0.06
STRI	-0.21	-0.28

The AGCD provides a new opportunity to examine in more detail the relationship between the 1888 Centennial Drought and Australia's climate drivers. The changing impacts of competing climate drivers on rainfall anomalies can be observed throughout the drought year, providing a comprehensive picture of the climatic factors that may have resulted in the 1888 Centennial Drought.

Table 2 shows the correlation of each index to rainfall in SEA at the time. Correlations are calculated for two relevant periods: firstly, for the Interdecadal Pacific Oscillation (IPO) phase which covered the drought (1880–1888) and secondly, for the 78-year climatology period. The IPO is a long-term climate oscillator whose phases represent SST anomalies in the tropical and subtropical Pacific Ocean and correspond to changes in surface temperature, rainfall, El Niño frequency and related phenomena (Dai et al. 2015; Kiem et al. 2003; Power et al. 1998; Wang et al. 2014). During the drought year 1888, the IPO was in its positive

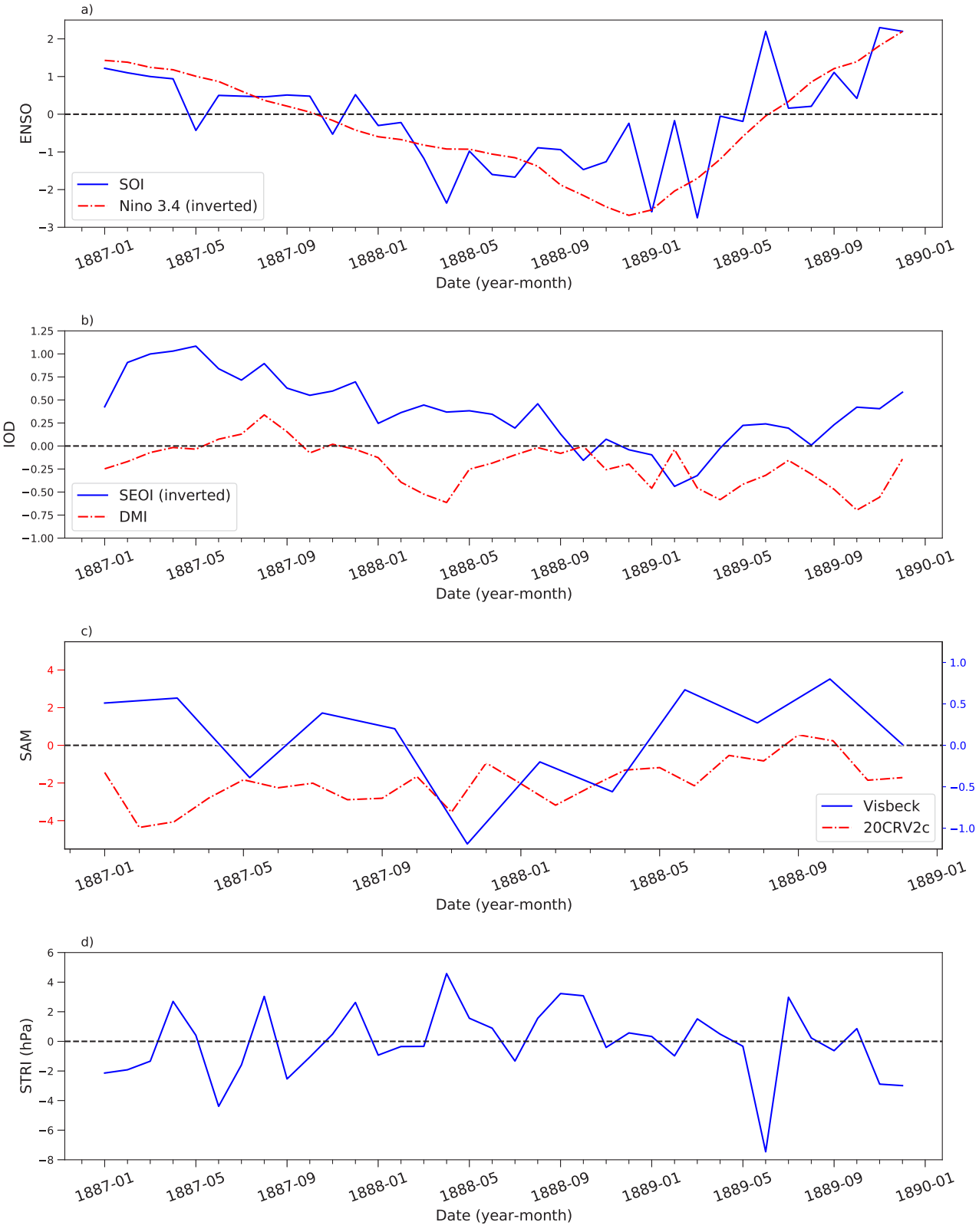

Figure 7: The following climate indices are plotted for the year 1887–1889 inclusive; time scale is monthly unless otherwise specified. a) Southern Oscillation Index (SOI) anomaly data from the Bureau of Meteorology, (2019c; in solid blue) and (inverted) Niño 3.4 anomalies (ºC; dashed red) derived from the HadISST dataset. A negative (inverted) Niño 3.4 or SOI anomaly indicates an El Niño event. b) Dipole Mode Index (DMI) anomalies (ºC) derived from the HadISST (solid blue) and (inverted) South Eastern Oscillation Index (SEOI) data (ºC; dashed red). A negative DMI or SEOI indicates a negative phase Indian Ocean Dipole. c) The Southern Annular Mode (SAM) index from Visbeck (2008; quarterly, solid blue) and from 20th century Reanalysis (20CRV2c; red dashed). Negative oscillations indicate negative phase SAM. d) The Sub Tropical Ridge Intensity (STR-I) anomalies, in solid blue.

phase, which typically indicates dominance of El Niño-like conditions in the Pacific Ocean and weaker correlations between ENSO and Australian rainfall (McGregor et al. 2010; Power et al. 1999, 2006). Given the relatively short duration of the IPO phase (eight years), correlations for the longer climatology period (1888–1965) are also considered for each index.

Widespread rainfall reductions in October–November 1888, as observed in both datasets, may be directly related to the onset of an El Niño event in the late winter months. The occurrence of an El Niño is indicated by both the Niño 3.4 index and the SOI. Typically, both indices are strongly correlated to rainfall in these months (Risbey et al. 2009) and both the SOI and the Niño 3.4 index are reasonably correlated to rainfall in SEA throughout the IPO phase, which covered the drought, as well as the longer climatology period (Table 2).

A (weak) negative IOD event later in the year may have also had some influence on rainfall throughout 1888. The DMI and SEOI also both show reasonable correlation to rainfall throughout the IPO phase (absolute values 0.32–0.36). Generally, a negative phase during the June–October period is associated with increased precipitation across southern Australia, including southwestern Victoria (Ashok et al. 2003; Risbey et al. 2009). However, the development of the strong El Niño may have dampened or negated the influence of the IOD at this time. Despite this, the signal of the negative DMI may be represented by the anomalous rainfall increases observed for substantial regions of the southwestern Victorian coast in early winter (see Figures 6F, G), as rainfall in this region is highly correlated with DMI variations in the cooler months (Risbey et al. 2009). However, as discussed previously, data issues and the conflicting indications of the DMI and SEOI early in the year suggest that the influence of the IOD on the Centennial Drought is uncertain.

Rainfall in southwestern parts of SEA can also be influenced by variations of the SAM. A positive SAM phase from December 1887 to March 1888 may account for the reduced rainfall seen in the southwestern corner of Tasmania in February, as the associated contraction of the westerly wind belt suppresses the northward intrusion of the rain-bearing frontal systems. The positive phase at this time may also explain the extreme rainfall increases over northeastern SEA, as the contraction of the belt supports enhanced onshore flow in this region (Hendon et al. 2007).

By autumn, the correlations between SAM and rainfall for SEA are significantly reduced (Hendon et al. 2007; Risbey et al. 2009), and hence unlikely to be the source of the strong autumn rainfall declines. A negative SAM phase during winter and spring is associated with increased precipitation for the southwestern Victorian coast, decreased precipitation in eastern SEA and increased precipitation in southwestern Tasmania (Hendon et al. 2007; Risbey et al., 2009). Each of these trends is observed in the Centennial Drought, supporting the conclusion that the SAM may have been a strong contributor to rainfall patterns at the time.

However, annual correlations during 1880–1888 are not strong. This is not unexpected, as the spatial variability and seasonality of the SAM's impact on rainfall in SEA (e.g. negative phase increases rainfall in New South Wales and decreases rainfall in Victoria) would result in a confused average. The relatively high frequency of oscillations may also contribute to the low correlation, as the low frequency of historical data fails to capture the completeness of the SAM variability. As a result, it is unlikely that, with these methods, statistical evidence for the SAM being a driver of the drought could be found. This could be a future focus of historical climate studies once more data become available.

Given the possible data issues in the SAM indices, the 20CRV2 signals were further interrogated, finding that the spatial distribution of pressure anomalies during the drought agree with the likely development of a negative phase. This, the Visbeck (2009) data and the distribution of rainfall anomalies throughout the drought discussed previously all suggest that the SAM was a significant contributor to rainfall variations in 1888.

During autumn, winter and spring, STR-I is negatively correlated with southern Australian rainfall (e.g. Timbal & Drosdowsky 2013), hence providing a potential explanation for the extreme rainfall declines observed in April 1888. The STR-I was also reasonably correlated to rainfall during both the IPO phase and the longer anomaly period, supporting this hypothesis. The negative correlation would result from the fact that, during autumn, the STR is situated over southern Australia at around 35° south (Pepler et al. 2018), meaning increased atmospheric pressure at this time would suppress the northerly intrusion of frontal systems and ultimately cut SEA off from the associated rainfall.

Comparison between the Centennial Drought and other short droughts

To provide context for the Centennial Drought, other short-lived drought events in SEA that stand out in the historical and modern record were examined. The 1914–15 drought was short and devastating, and is reported to have caused widespread rainfall declines across large regions of eastern Australia (Bureau of Meteorology 2020b). The May–October period of 1914 remains the driest on record for large areas of southern Australia, and the Murray River at Echuca fell to its lowest then recorded level (Bureau of Meteorology 2020b).

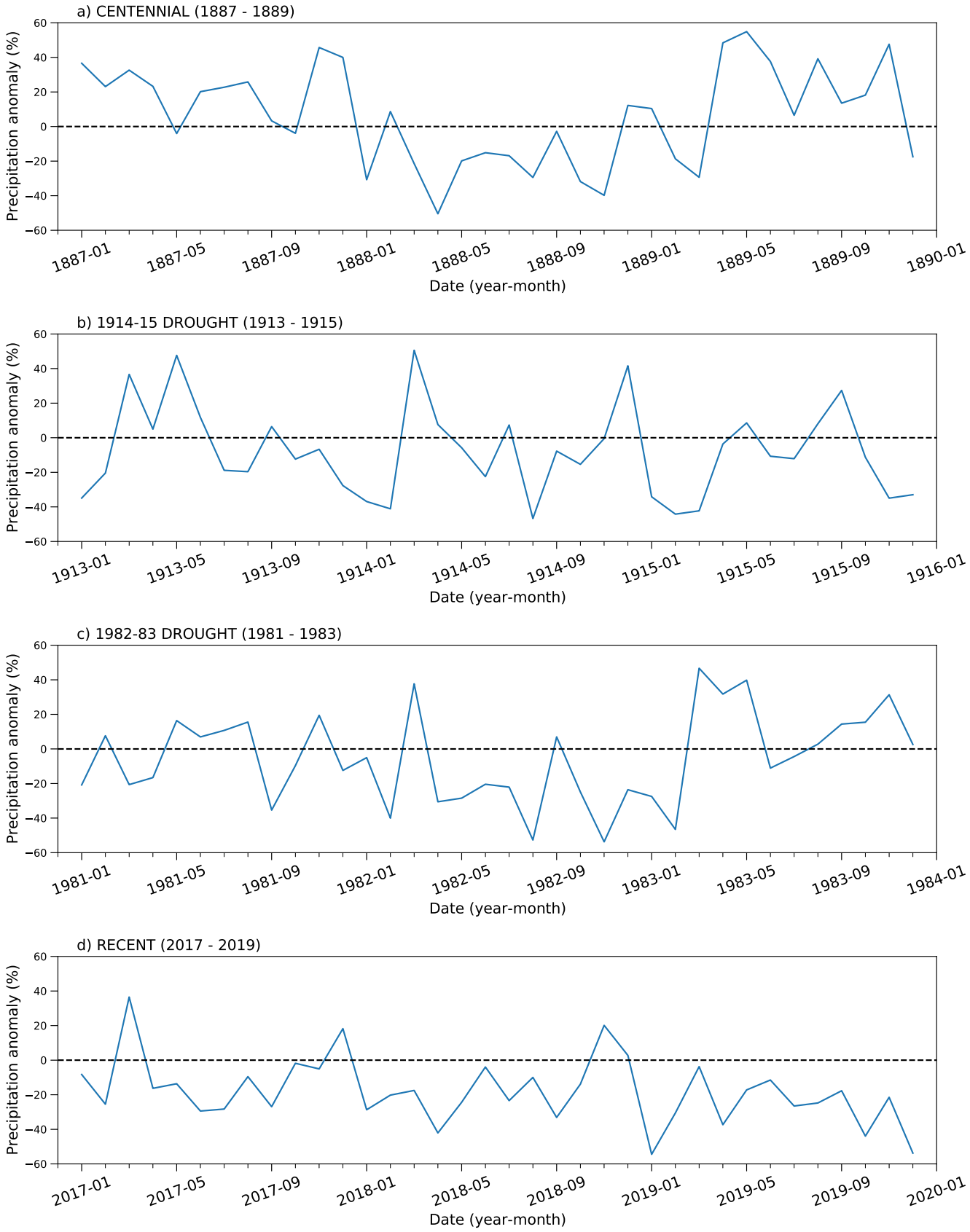

Figure 8: Monthly rainfall anomalies (%) for SEA relative to the period 1888–1965 for a) the Centennial Drought (1887–89), b) the 1914–15 drought (1913–1915) c) the 1982–83 drought (1981–1983) and d) the recent drought (2017 – 2019).

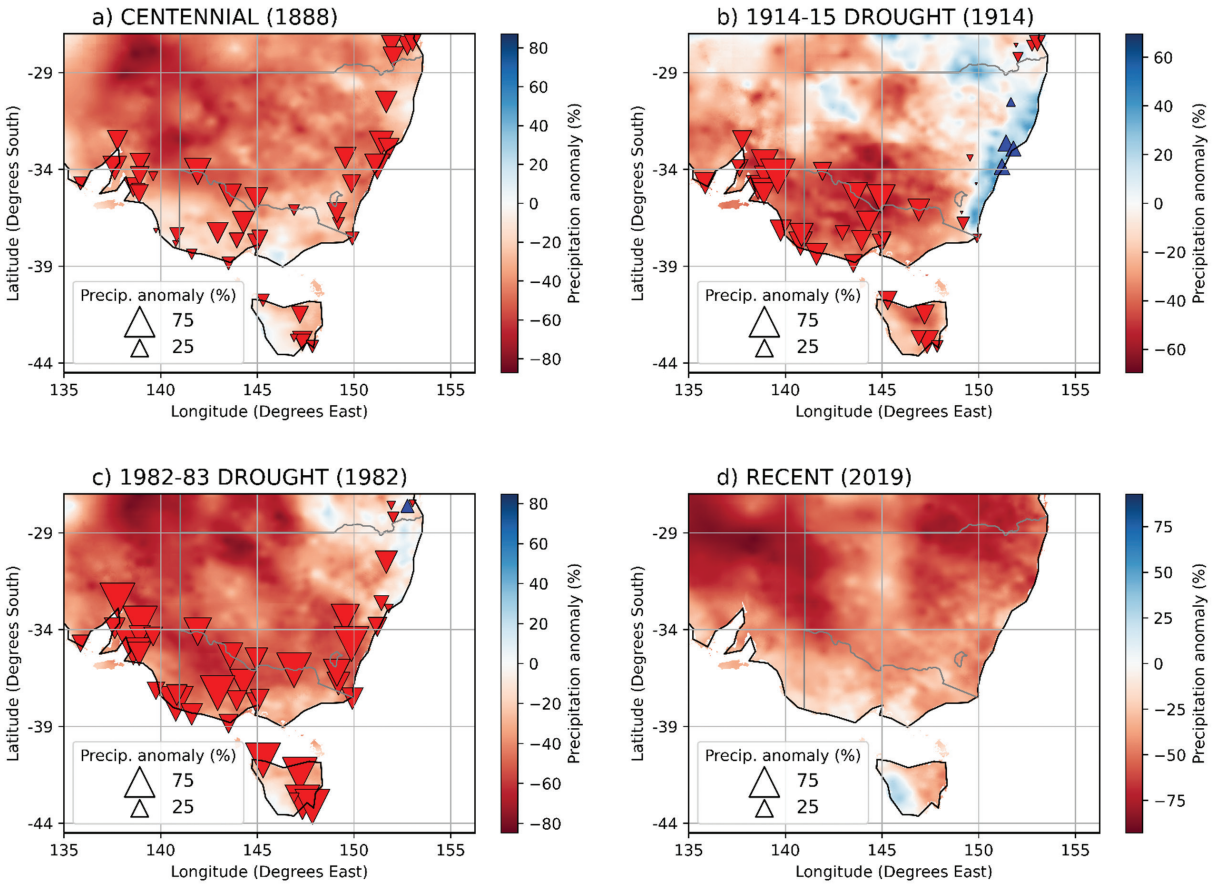

Figure 9: Annual (12-month period starting in January) spatial distribution of rainfall anomalies (%) across SEA relative to the period 1888–1965. Gridded climate data is shaded, and the station network is represented by triangles. a) the Centennial Drought (1888), b) the 1914–15 drought (1914) c) the 1982–83 drought (1982) and d) the recent drought (2018).

Figures 8B and 9B show that rainfall declines of 1914 and 1915 were indeed severe. The wet conditions of early autumn and late summer in 1914 failed to compensate for the dry winter and spring, with annual rainfall anomalies for the year very much below average throughout most of SEA. The seasonality of the drought through 1914 bears some resemblance to that of 1888, the main difference being in autumn, where 1888 is very dry and 1914 is closer to the long-term average. Spatially, the droughts have less in common on the annual scale, with a wet region along the eastern coast in 1914 not being represented annually in 1888. A similar pattern, however, is observed in September and October of 1888.

The 1914 drought has been attributed to a strong El Niño event (Bureau of Meteorology 2020b); this is evidenced in both the SOI and Niño 3.4. In addition to a strong El Niño, there was a particularly high magnitude STR-I anomaly throughout the year, potentially exacerbating the already dry conditions. The influence of ENSO on this drought — and on the Centennial Drought — may explain the eastern coast wet region observed in the year of 1914 and the spring of 1888, since, on average, this region does not observe the rainfall declines that an El Niño drives for the rest of SEA (Bureau of Meteorology 2014).

Another short, yet extreme, drought that devastated SEA was the 1982–83 drought (Figures 8C, 9C), which is reported to be one of Australia's most severe droughts of the 20th century (Bureau of Meteorology 2020b). Previous analysis by Gibbs (1984, p. 92) describes a year in which sharp downturns were observed in wheat production, sheep and cattle populations, topsoil, reservoir reserves, power generation and the national economy: 'Practically all highly urbanized areas … were in the grip of one of the worst droughts in almost 200 years of European settlement of the continent.' Gibbs further suggests that the 1982 drought is comparable in severity to the Centennial, in agreement with the conclusion in this analysis, which shows that the monthly rainfall anomalies for both droughts from April to November were between 20 and 40% below average. Spatially, the two drought years exhibit very similar signatures, with both droughts showing extreme precipitation declines across all of SEA on the annual scale. The sharpest declines for both are reported inland, in western New South Wales and eastern South Australia, and some regions of closer-to-normal rainfall conditions are seen along the eastern coast.

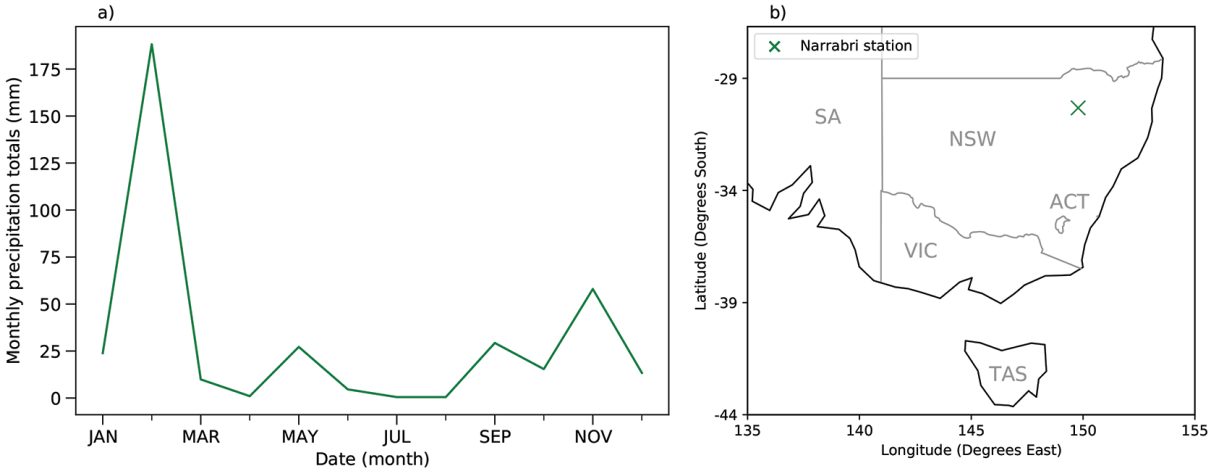

Figure 10: a) Total monthly precipitation (mm) for Narrabri station in 1888. b) Geographic location of Narrabri station.

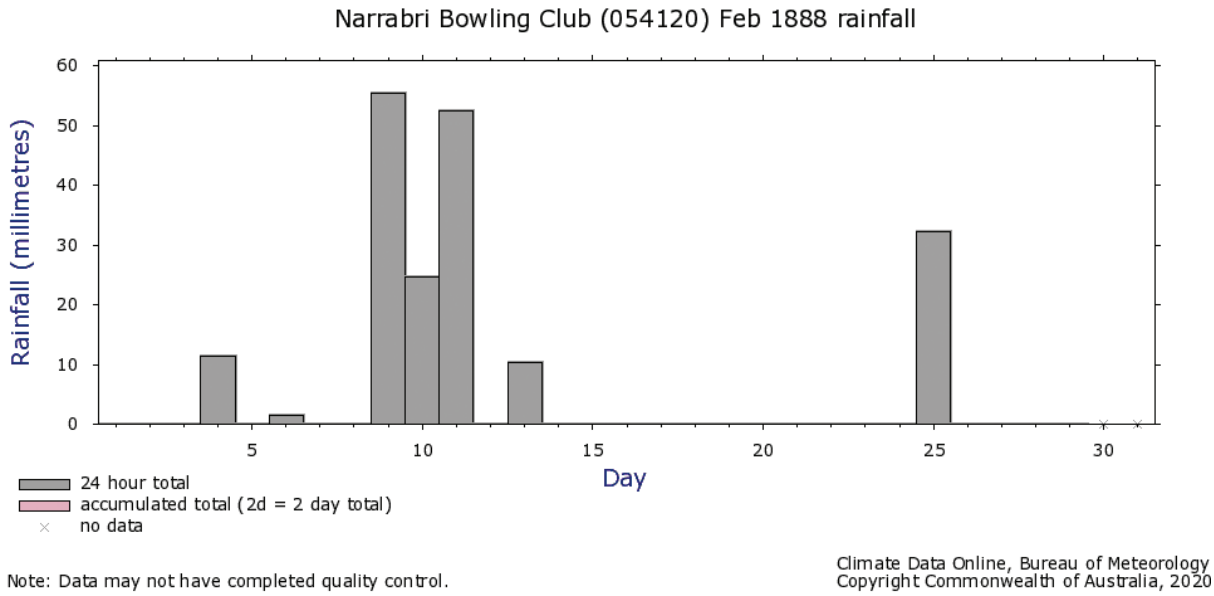

Figure 11: Daily total precipitation (mm) for Narrabri station in February 1888 (Bureau of Meteorology 2020d).

As with 1914, the 1982 drought has been attributed to a strong El Niño event (Bureau of Meteorology 2020b). A particularly strong El Niño signal does arise in both indices, along with a positive IOD event, which is also indicated by both the DMI and SEIO (not shown). The occurrence of an El Niño and positive phase IOD event together can result in exaggerated rainfall declines across Australia (Risbey et al. 2009).

The recent drought, starting in 2017 and ongoing in some areas, is another short, intense drought that has impacted SEA (Figures 8D, 9D). The three-year period from 2017–2019 inclusive was the driest on record (records for three-year intervals from January, starting in 1900) for the Murray–Darling Basin and New South Wales. The monthly evolution of the recent drought shows rainfall around 20% below average for almost the entirety of 2018 and 2019. The second half of 2019 saw even more extreme declines, with the later months seeing just 50% of their average totals. Despite a lower range of inter-month variability, the evolution of the drought through 2018 and 2019 is comparable to that of 1888, which saw similar magnitude declines but with some relief in February and September.

The duration of the recent drought was also greater than the three others considered. Spatially, the signature is similar to both 1888 and 1982, with the exception of eastern New South Wales and Queensland, where the recent drought saw more extreme drying. Rather than an El Niño, as was the case for 1888 and 1982, the recent drought resulted from one of the strongest positive IOD events on record, along with a persistent negative phase SAM (Bureau of Meteorology 2020b).

Data comparison

As this is the first time the AGCD has been used to examine an historical drought in detail, it is worth examining the agreement and disagreements between the gridded and observational datasets. In general, spatial agreement is impressive between the AGCD and the historical station network, with both agreeing on multiple regional events as well as large-scale variability. This suggests that a well-spaced network of stations can accurately capture, at least at the monthly scale, regional rainfall patterns in the historic period. This is a valuable finding for future studies of droughts that occurred in the pre-1880 period.

The strongest disagreement between the datasets arises during extremely dry or wet months, with the station network data tending to show larger anomalies than the AGCD. The spatial representations shown in Figure 6 provide some explanation of the disagreement. For example, February 1888 shows strong disagreement, with the AGCD apparently exaggerating a minor positive trend observed in the station network. However, Figure 6B shows AGCD capturing above average rainfall for a large region of inland north eastern SEA that is not represented by the station network.

To explore this discrepancy further, we sourced daily and monthly precipitation data from Narrabri, in the region of the high rainfall captured by AGCD (Bureau of Meteorology station number 054120; Bureau of Meteorology 2020d). The data during 1888 (Figures 10, 11) show a short (three-day) period of extreme rainfall interrupting an otherwise dry month. The data are incorporated into the AGCD product and therefore influence the gridded output for the region. However, Narrabri was not included in the 42-station network, thus indicating that differences in input data likely explain disagreement between the datasets.

The AGCD provides clear depictions of regional precipitation patterns throughout 1888 which are largely supported by the station observations. This is valuable, as a reliable map of rainfall patterns allows for more comprehensive reviews of the potential causes of a drought. For the Centennial Drought, this is clear in the SAM signals in November and February, which saw rainfall anomalies that align well with the regions of strongest SAM–rainfall correlation (Risbey et al. 2009).

In months where precipitation anomalies are less extreme, such as May, September and December, the AGCD product provides opportunity to observe less pronounced and/or higher resolution rainfall patterns that are not as well captured by the, largely coastal, 42-station network.

CONCLUSION

This study presents a quantitative analysis of the Centennial Drought of 1888, showing significant declines in autumn, winter and spring rainfall that were likely due to a combination of an El Niño event, the SAM and a positive STR-I anomaly. The extreme declines of 1888, along with the widespread reach of the short, sharp drought, are comparable to the historic droughts of 1914 and 1982 as well as the recent drought of 2017–2019. Separate analysis by two datasets — a 42-station network of historic instrumental observations and a newly developed high-resolution gridded climate data product — produced strong agreement on the drought characteristics, both spatially and temporally.

This work extends our understanding of Australia's drought history by capturing the spatial extent, duration, evolution and severity of the historical 1888 Centennial Drought. The relatively short instrumental record limits the number of droughts in Australia's climate history whose nature and causes are well understood. The addition of the Centennial Drought to these numbers will aid future scenario modelling for Australia's climate adaptation, which, as Australia's climate continues to change and its droughts change with it, can only improve our understanding of future conditions.

Acknowledgements

We acknowledge that we have been undertaking this work on the lands of the Wurundjeri people of the Kulin Nation and that this research concerns the country of many more sovereign nations and we pay our respects to Elders past, present and emerging.

We also thank Alex Evans and Robert Smalley from the Bureau of Meteorology for their assistance and generosity in sharing the AGCD data, and Scott Wales from the ARC Centre of Excellence for Climate Extremes for his technical support. We are grateful to two anonymous reviewers whose comments improved this manuscript. This research was supported by an undergraduate summer scholarship from the ARC Centre of Excellence for Climate Extremes (CE170100023).

Conflict of interest

The authors declare no conflicts of interest.

References

Abram, N.J., Dixon, B.C., Rosevear, M.G., Plunkett, B., Gagan, M.K., Hantoro, W.S. & Phipps, S.J., 2015. Optimized coral reconstructions of the Indian Ocean Dipole: an assessment of location and length considerations. *Paleoceanography* 30: 1391– 1405.

Allan, R.J. & Haylock, M.R., 1993. Circulation features associated with the winter rainfall decrease in Southwestern Australia. *Journal of Climate* 6: 1356–1367.

Ashok, K., Guan, Z. & Yamagata, T., 2003. Influence of the Indian Ocean dipole on the Australian winter rainfall. *Geophysical Research Letters* 30(15): 1821.

Bridgman, H., Ashcroft, L., Thornton, K., Di Gravio, G. & Oates, W., 2019. Meteorological observations for Eversleigh Station, near Armidale, New South Wales, Australia: 1877–1922. *Geoscience Data Journal* 6: 174–188.

Bureau of Meteorology, 2014. *What is El Niño and What Might it Mean for Australia?* Available at: http://www.bom.gov.au/climate/updates/articles/a008-el-Niño-and-australia.shtml (Accessed 05/10/2020).

Bureau of Meteorology, 2019. *Special Climate Statement 70: Drought Conditions in eastern Australia and Impact on Water Resources in the Murray–Darling Basin*. The Australian Bureau of Meteorology. Available at: http://www.bom.gov.au/climate/current/statements/scs70.pdf.

Bureau of Meteorology, 2020a. *Drought Statement: Above Average August Rainfall Lessens Some Short-term Deficiencies, but Little Relief in WA*. The Australian Bureau of Meteorology. Available at: http://www.bom.gov.au/climate/drought/archive/20200908.archive.shtml (Accessed: 26/09/2020).

Bureau of Meteorology, 2020b. *Previous Droughts. The Australian Bureau of Meteorology*. Available at: http://www.bom.gov.au/climate/drought/knowledge-centre/previous-droughts.shtml (Accessed: 04/10/2020).

Bureau of Meteorology 2020c. *Average Annual, Seasonal and Monthly Rainfall*. The Australian Bureau of Meteorology. Available at: http://www.bom.gov.au/jsp/ncc/climate_averages/rainfall/index.jsp (Accessed: 13/10/2020).

Bureau of Meteorology, 2020d. *Recent and Historical Rainfall Maps*. The Australian Bureau of Meteorology. Available at: http://www.bom.gov.au/climate/drought/#tabs=Rainfall-tracker (Accessed 16/07/2020).

Dai, A., Fyfe, J., Xie, S. & Dai, X., 2015. Decadal modulation of global surface temperature by internal climate variability. *Nature Climate Change* 5: 555–559.

Dey, R., Lewis, S.C., Arblaster, J.M. & Abram, N.J., 2019. A review of past and projected changes in Australia's rainfall. *Wiley Interdisciplinary Reviews: Climate Change*. John Wiley & Sons, Ltd, 10(3): e577.

Drosdowsky, W., 2005. The latitude of the subtropical ridge over eastern Australia: the L index revisited. *International Journal of Climatology* 25: 1291–1299.

Evans, A., Jones, D., Smalley, D. & Lellyett, S., 2020. *An Enhanced Gridded Rainfall Dataset Scheme for Australia*, Bureau Research Report No. 041. Available at http://www.bom.gov.au/research/publications/researchreports/BRR-041.pdf.

Fenby, C. & Gergis, J., 2013. A rainfall history of south-eastern Australia Part 1: a consolidation of pre-instrumental evidence from documentary sources, 1788–1860. *International Journal of Climatology* 33: 2956–2972.

Gergis, J. & Ashcroft, L., 2013. Rainfall variations in south-eastern Australia part 2: a comparison of documentary, early instrumental and palaeoclimate records, 1788–2008. *International Journal of Climatology* 32(14).

Gibbs, W. & Maher, J., 1967. Rainfall Deciles as Drought Indicators. The Australian Bureau of Meteorology.

Gibbs, W., 1984. The great Australian drought: 1982–1983*. *Disasters* 8: 89-104.

Glenmaggie, M., 1888. DROUGHT. *The Gippsland Farmers' Journal and Traralgon, Heyfield and Rosedale News*. p. 3. Available at: http://nla.gov.au/nla.news-article227348296.

Gong, D. & Wang, S., 1999. Definition of Antarctic Oscillation index. *Geophysical Research Letters* 26: 459–462.

Helman, P., 2009. *Droughts in the Murray–Darling Basin Since European Settlement*. Griffith University, Southport.

Hendon, H., Thompson, D. & Wheeler, M., 2007. Australian rainfall and surface temperature variations associated with the southern annular mode. *Journal of Climate* 20: 2452–2467.

Holgate, C.M., Van Dijk, A.I.J.M., Evans, J.P. & Pitman, A.J., 2020. Local and remote drivers of Southeast Australian Drought. *Geophysical Research Letters* 47(18).

Jones, D.A., Wang, W. & Fawcett, R., 2009. High-quality spatial climate datasets for Australia. *Australian Meteorological Magazine* 58:233–248.

Kiem, A. S., Franks, S.W. & Kuczera, G., 2003. Multi-decadal variability of flood risk. *Geophysical Research Letters* 30: 1035.

Kiem, A.S. & Verdon-Kidd, D.C., 2010. Towards understanding hydroclimatic change in Victoria, Australia: preliminary insights into the 'Big Dry'. *Hydrology and Earth System Sciences* 14: 433–445.

Larsen, S. & Nicholls, N., 2009. Southern Australian rainfall and the subtropical ridge: variations, interrelationships, and trends. *Geophysical Research Letters* 38(8).

Li, Z., Cai, W. & Lin, X., 2016. Dynamics of changing impacts of tropical Indo-Pacific variability on Indian

and Australian rainfall. *Scientific Reports* 6: 31767.

McBride, J. & Nicholls, N., 1983. Seasonal relationships between Australian rainfall and the Southern Oscillation. *Monthly Weather Review* 111: 1998–2004.

McGregor, S., Timmermann, A. & Timm, O., 2010. A unified proxy for ENSO and PDO variability since 1650. *Climate of the Past* 6: 1–17.

Meyers, G., McIntosh, P., Pigot, L. & Pook, M., 2007. The years of El Niño, La Nina, and interactions with the tropical Indian Ocean. *Journal of Climate* 20: 2872–2880.

Murphy, B.F. & Timbal, B., 2008. A review of recent climate variability and climate change in Southeastern Australia. *International Journal of Climatology* 28(7): 859–879.

Nicholls, N., 1987. El Niño Southern Oscillation and rainfall variability. *Journal of Climate* 1: 418–421.

Nicholls, N., 1989. Sea surface temperature and Australian winter rainfall. *Journal of Climate* 2: 965–973.

Nicholls, N., 1997. The Centennial Drought, in *Windows on Meteorology: Australian Perspective*. E.K. Webb, ed. CSIRO Publishing, Melbourne, pp 118–127.

Nicholls, N., 2010. Local and remote causes of the southern Australian autumn–winter rainfall decline, 1958–2007. *Climate Dynamics* 34: 835–845.

Pepler, A., Ashcroft, L. & Trewin, B., 2018. The relationship between the subtropical ridge and Australian temperatures. *Journal of Southern Hemisphere Earth Systems Science* 68: 201–214.

Power, S., Tseitkin, F., Torok, S., Lavery, B., Dahni, R. & McAvaney, B., 1998. Australian temperature, Australian rainfall and the Southern Oscillation, 1919–1992: coherent variability and recent changes. *Australian Meteorological Magazine* 47: 85–101.

Power, S., Casey, T., Folland, C., Coleman, A. & Mehta, V., 1999. Inter-decadal modulation of the impact of ENSO on Australia. *Climate Dynamics* 15: 319–324.

Power, S., Haylock, M., Colman, R. & Wang, X., 2006. The predictability of interdecadal changes in ENSO activity and ENSO teleconnections. *Journal of Climate* 19: 4755–4771.

Rayner, N., Parker, D., Horton, E., Folland, C., Alexander, L., Rowell, D., Kent, E. & Kaplan, A., 2003. Global analyses of sea surface temperature, sea ice, and night marine air temperature since the late nineteenth century. *Journal of Geophysical Research: Atmospheres* 108(D14).

Risbey, J., Pook, M., McIntosh, P., Wheeler, M. & Hendon, H., 2009. On the remote drivers of rainfall variability in Australia. *Monthly Weather Review* 137(10): 3233–3253.

Saji, N., Goswami, B., Vinayachandran, P. & Yamagata, T., 1999. A dipole mode in the tropical Indian ocean. *Nature* 401(6751): 360–363.

Thompson, D. & Solomon, S., 2002: Interpretation of recent southern hemisphere climate change. *Science* 296: 895–899.

Timbal, B. & Drosdowsky, W., 2013. The relationship between the decline of Southeastern Australian rainfall and the strengthening of the subtropical ridge. *International Journal of Climatology* 33(4): 1021–1034.

Timbal, B. & Fawcett, R., 2013. A historical perspective on Southeastern Australian rainfall since 1865 using the instrumental record. *Journal of Climate* 26(4): 1112–1129.

Trenberth, K. & National Center for Atmospheric Research Staff, 2019. *The Climate Data Guide: Niño SST Indices (Niño 1+2, 3, 3.4, 4; ONI and TNI)*. Available at: https://climatedataguide.ucar.edu/climate-data/Niño-sst-indices-Niño-12-3-34-4-oni-and-tni (Accessed: 23/09/2019).

Ummenhofer, C.C., England, M.H., Mclntosh, P.C., Meyers, G.A., Pook, M.J., Risbey, J.S., Gupta, A.S. & Taschetto, A.S., 2009. What causes southeast Australia's worst droughts?. *Geophysical Research Letters* 36: L04706.

Verdon-Kidd, D.C. & Franks, S.W., 2005. Indian Ocean sea surface temperature variability and winter rainfall: Eastern Australia. *Water Resources Research* 41: W09413.

Verdon-Kidd, D.C. & Kiem, A.S., 2009. Nature and ca uses of protracted droughts in southeast Australia: comparison between the Federation, WWII, and Big Dry droughts. *Geophysical Research Letters* 36 (22): L22707.

Visbeck, M., 2009. A station-based Southern Annular Mode Index from 1884 to 2005. *Journal of Climate* 22: 940–950.

Wang, S., Huang, J., He, Y. & Guan, Y., 2014. Combined effects of the Pacific Decadal Oscillation and El Niño-Southern Oscillation on Global Land Dry–Wet Changes. *Scientific Reports* 4: 6651.